Natural Hazards (2024) 120:4083–4100
https://doi.org/10.1007/s11069-023-06371-6

ORIGINAL PAPER

Unravelling increasing flood hazard and influential factors in a tidal river

Yao Wu[1,2,3,4] · Wei Zhang[1,4] · Xiaozhang Hu[2,3] · Chen Lu[2,3,5] · Shiyou Gao[2,3]

Received: 20 April 2023 / Accepted: 5 December 2023 / Published online: 4 January 2024

Abstract

Flood disasters are destructive especially in prosperous and urbanized estuarine regions, where the flood regime is much more complex due to multiple fluvial–estuarine impacts. The Shenzhen River (SZR), located in one of the most prosperous regions of southern China, is vulnerable to increasing flood risk. Unravelling the influential factors is of particular significance to flood hazards prevention and urban safety for the SZR. Based on the field-measured floods on June 13, 2008 ("2008.06") and August 29, 2018 ("2018.08") with roughly equal magnitudes of rainfall and tide, the changing flood risk in the SZR basin was assessed. Considering the substantial development of tidal flat plants in the past two decades, a physical model of the SZR was built to quantify the impacts of changing river regime on the flood stage. The model covers the whole mainstream of tidal reach and half of the Shenzhen Bay (SZB), which was well calibrated and validated by in situ flow process. Several situations with different ranges of riverine vegetation and estuarine mangrove, including all vegetation (actual situation), half vegetation, no vegetation, mangrove in 2002 and 2018, were modelled to explore flood stage variations in 2-yr and 50-yr return period. The results found that the "2018.08" flood stage was about 1.4 m higher than "2008.06" flood. Moreover, the rainfall–runoff duration in "2018.08" was significantly decreased by 1 h less than that of "2008.06" flood, indicating increased flood risk in the SZR. The flood stage in the middle reach increases by more than 0.6 m driven by the riverine vegetation during the 50-yr return period flood, while the flood stage rises less than 0.1 m for the flood with 2-yr return period. Moreover, the extended estuarine mangrove forest resulted in about 0.2 m flood stage increment in the lower reach. The effects of sea level rise and sediment deposition after channel dredging on the flood risk in the SZR were further discussed. The effects of sea level rise and sediment deposition after channel dredging on flood risk were further discussed in the SZR. Channel infilling probably causes a flood stage increase of approximately 0.5 m for all reaches, while the influence of sea level is relatively slight but cumulative. Sufficient river management and planning, such as seasonal removal of riverine vegetation, mangrove management and regular topography surveys, should be taken into consideration in the near future.

Keywords Flood risk · Riverine vegetation · Influence factors · Physical model · Tidal river

Extended author information available on the last page of the article

1 Introduction

Flood disasters are prevalent and devastating in many parts of the world, with remarkable life loss, property damage and essential services disruption (Wang et al. 2021). Since estuarine regions are generally characterized by prosperous socioeconomic activity and high population density considering efficient maritime transportation and access to rich natural resources (Wu et al. 2018; Vousdoukas et al. 2018), flood hazards are particularly destructive for highly urbanized tidal river estuaries, resulting in countless economic and social impacts. In recent decades, extreme weather events triggered by global warming have driven rising flood risk. Nuisance flooding is susceptible to increasing heavy precipitation events, with the trend of magnitude and frequency expected to worse in the future (Moftakhari et al. 2016). Especially for a tidal river estuary, global warming has the potential to induce sea level rise and the enhancement of tropic cyclones. These climate extremes pose a more severe challenge to flood protection in tidal river systems (Xie et al. 2021).

Since low-lying tidal river regions are generally occupied by human, intensive anthropogenic interventions are closely related to the changing flood regime, which may be responsible for the increasingly potential flood risk (Orton et al. 2018). Social development has significantly transformed the physical setting, such as channel dredging and infilling, sand excavation, land reclamation, shorelines hardening, cross-river bridges construction, diversion channels shrinkage and connecting lake contraction (Fan et al. 2008). These geomorphological changes are expected to alter hydrodynamics and sediment transport, leading to the modification of tidal pumping effect and flood-carrying capacity in tidal river systems (Ralston et al. 2019). For the purpose of improving navigation condition, channel dredging is conducted commonly, while remarkable sediment deposition is found shortly afterwards. Since substantive channel deepening destabilizes the equilibrium state of tidal river system, the sediment-carrying capacity of flow is undermined with more sediment trapped (Wu et al. 2020). Flood risk is thus enhanced accompanying with the process of channel infilling. Furthermore, due to the great demand of land use, extensive land reclamation projects have been implemented. The fluvial–tidal flow is probably concentrated and intensified as the river outlet is narrowed with numerous intertidal areas occupied, which is highly linked to the increasing flood risk (He et al. 2019). Additionally, construction of levees isolate floodplain from flood flow constrained in rivers along with streamside urbanization development. Such anthropogenic modifications have been proved to be critical to flood hazard in tidal rivers (Jian et al. 2020).

Apart from the impact of anthropogenic interferences, the formation and extension of riparian vegetation also can introduce conspicuous flood risk. Generally, various types of riparian vegetation are conductive to habitat condition for organisms, water quality and aesthetic appeal (Hey and Thorne 1986) improving the habitat conditions for organisms, which satisfies the demand of ecological protection policy. Additionally, riparian vegetation also has the potential to enhance bank stability by reducing near-bank tidal velocity and soil moisture content (Darby 1999). However, the disorder growth and expansion of riparian vegetation can lead to significantly detrimental effect, especially the potential risk of flooding due to the increasing flow resistance. The magnitude of flow resistance is reliant on various complex factors, including the species, extent, age and the physical properties of the riparian vegetation, which poses obvious impacts on flood stage especially at flood sensitive sites. A vast literature has unravelled the influence of riparian vegetation on flow resistance in fluvial system, while tidal river reaches were received relatively less attention (Fernandez et al. 2021). Researches about flow

resistance based on resistance equation for short submerged vegetation and tall non-submerged vegetation are distinct (Fathi-Moghadam et al. 2011). Detailed numerical models (Shimizu and Tsujimoto 1994), analytical approaches (Masterman and Thorne 1994) and flume experiments (Kouwen and Fathi-Moghadam 2000) have been applied on detecting the interaction between vegetations stems and flow condition. For tidal river estuaries, the flow resistance varies with tidal level since it highly associates with the submerged height of riparian vegetation. During the flood period, the flood stage has the potential to significantly alter in magnitude, indicating that the flow resistance can be variable in the flood process. To our knowledge, the interplay between vegetation and changing resistance, relating with the accurate calculation of flood stage, is becoming an increasingly important task but is not yet well documented (Wang et al. 2015).

The Shenzhen River (SZR), as the border of Shenzhen and Hong Kong, locates at one of the most prosperous regions of the southern China (Fig. 1). Flood events used to pose a challenge to the SZR and nearby urban area before 1995, since its mainstream was meandering and shallow. In order to improve the flood prevention standard to 50-year return period, a cascade of river regulation projects, mainly channel dredging and embankments heightening, were conducted to lower flood stage, which has played an important role on keeping people from flood hazards and promoting regional economic development (Wu et al. 2020). As a result of extreme weather and anthropogenic interferences, flood risk at the SZR tends to aggravate. Therefore, the flood prevention standard at the SZH has been undermined in the past several years.

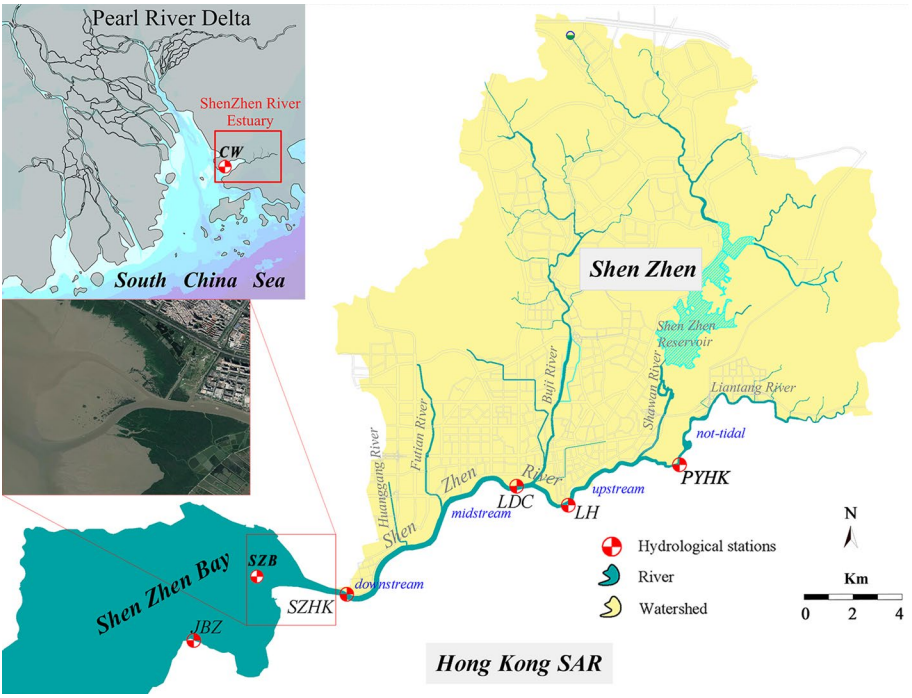

Fig. 1 Location of the study area in the Pearl River Delta, southern China and the Shenzhen River Basin

In this paper, the changing pattern of flood risk and influence factors of flood stage at SZR were explored. Firstly, we will detect the changing flood stage and precipitation regime based on field-measured hydrological and meteorological data. Then, a physical model involving the SZR and the Shenzhen Bay (SZB) was built to assess the impacts of in-channel riparian vegetation and estuarine mangrove forest on the flood stage of the SZR. Furthermore, the implication of channel infilling and sea level rise on flood hazard was discussed. Assessing the potential influence factors of flood stage provides further insight into relieving river regulation burdens and making prospective flood prevention policy, which is conductive to reducing its impacts on life and property in a tidal river system.

2 Study area and data

The SZR is a small tidal river with 312.5 km^2 drainage area in the Pearl River Delta, located at the southern China (Fig. 1). Its mainstream is the border of Shenzhen and Hong Kong, both of which are highly economic developed metropolis (Zhang and Mao 2015). Considering the important geographical location, the flood prevention ability of the SZR urgently needs to be enhanced. The river basin is characterized by fan-shaped with seven main tributaries. The slope of tributaries is about 2–4‰ while the slope of mainstream is only 0.2–0.5‰, partly leading to high flood risk of the SZR. Additionally, about 13 km mainstream is influenced by tidal impact, indicating that the flood risk is probably intensified when it encounters with the flood tide (Wu et al. 2020). Futian (Shenzhen) and Mipu (Hong Kong) Mangrove Nature Reserve are located at the semi-enclosed of SZB with about 3.7 million km^2 and 15 million km^2, respectively, both which are national mangrove nature reserves known for its mangrove trees and is a habitat for numerous endangered bird species (Luo et al. 2010; Ren et al. 2011). As the major wintering and stopover sites along migratory routes, about 50–80 thousand of birds with more than 440 species inhabit in the reserve. Due to the well protection, the area of mangrove has continuously extended from 259.6 to 527.1 ha during the period of 1988–2017, which tends to impede the release of flood discharge of the SZR (Wang et al. 2022).

Due to the global climate change, rainfall intensity in the SZR basin has been proved to be increased. Moreover, rapid urbanization process in Shenzhen also triggers rainfall–runoff duration alteration, which has the potential to increase regional flood risk (Ng et al. 2011; Fay et al. 2010). In recent years, the resident population in the SZR basin has already exceeded 2 million with more than 70 billion dollars Gross Domestic Product. Therefore, the flood prevention in the SZR should be put more attention. Before 1995, the SZR was only capable of conveying a flood of 2–5 years return periods with shallow and meandering channel. As a series of river trainings have been implemented in the past two decades, the ability of flood prevention is significantly improved (Chan and Lee 2010). According to the consecutive hydrological data attained from the Municipal Shenzhen River Regulation Office of Shenzhen (MSRRO), two significant rainstorm events with similar rainfall intensity and duration were found in the SZR basin after 2008, which happened in 13th June 2008 and 29th August 2018, namely "2008.06" and "2018.08" rainfall, respectively. In order to characterize the changing flood regime, field-measured data at several monitoring stations, such as precipitation, discharge and flood stage, were collected in this study.

3 Model description

3.1 Model set-up

A physical model has been built to quantify the impacts of changing river regime on the flood stage. Considering the limitation of model occupied area, the physical model is set as about 45 m in length and 14 m wide with a plane scale λ_l of 300. For the purpose of ensuring the accuracy of flow stage modelling and measurement, the vertical scale λ_h is set as 50, indicating that the scale ratio η is 6. In order to cover the mainstream of tidal reach, the upper boundary of the physical model is set at the PYHK station, upstream the tidal current boundary of the SZR (Fig. 1). The lower boundary is set at the JBZ station close to the middle part of the SZB, which is able to cover estuarine region and the Futian and Mipu natural mangrove reserves. The upper and lower boundary conditions of the physical model are, respectively, determined by the fluvial discharge process at the PYHK station and tidal signal at the JBZ station. The boundary conditions in 2-yr and 50-yr return periods have been studied by flood and tide frequency analysis based on long-term in situ hydrological data in the SZR. Furthermore, since climate change is expected to increase the frequency and intensity of extreme weather events, such as heavy precipitation, droughts and storm surge, boundary conditions in the model will be linked to any possible future scenario of high greenhouse gas emissions and global warming. How boundary conditions calculation and possible future flood variations associate with climate change needs to be further studied.

In order to simulate the changing fluvial and tidal process, flood flow and tidal flow are discharged into the model by submersible pump. The fluvial discharge is controlled by high precision electromagnetic flowmeter, flood flow at the upper boundary thus can be accurately monitored in the model (Gimbert et al. 2014). For the lower boundary, water level indicator cooperated with bidirectional submersible pump is employed to adjust the changing tidal level. Water flow is aspirated in order to raise the model tidal level since it is lower than the measured data in the prototype. On the contrary, water flow is expelled by the submersible pump when higher water level in the model is found. Generally, stable tidal process can be achieved about 20 min after the running of the model. According to the plane and vertical scale, the physical model is built by bricks and cement. Topographic maps in 2016 with the scale of 1:2000 in the SZR and 1:2500 in the SZB are applied to set the model geomorphology. Furthermore, based on the law of gravity similarity, the flow velocity scale λ_v is calculated as:

$$\lambda_v = \lambda_h^{1/2} = 7.07$$

Based on the law of resistance similarity, the roughness scale λ_n is calculated as:

$$\lambda_n = \lambda_h^{1/6}\left(\frac{\lambda_h}{\lambda_l}\right)^{1/2} = 0.784$$

while the time scale of flow is defined as:

$$\lambda_{t1} = \frac{\lambda_l}{\lambda_v} = 42.43$$

while the discharge scale is defined as:

$$\lambda_Q = \lambda_l \lambda_h \lambda_v = 106066$$

3.2 Model calibration and verification

Based on the field-measured water level, the physical model is calibrated and validated. Flow roughness, as an important parameter, associates with the simulation of the water level in the SZR. Especially during the flood period, flow roughness varies with the significant fluctuation of flood stage. Due to the influence of widespread riparian vegetation at the tidal flat, flow roughness of the SZR increases with the rise of flood stage. Higher flood stage tends to result in larger flow roughness since more riparian vegetation is submerged.

In this study, flow roughness of tidal flat produced by riparian vegetation is simulated by the plastic grass according to the highness and density of riparian vegetation, which is similar to the roughness characteristics of the riverine plant. Roughness of riverbed is simulated by the plastic bar with various heights. For the purpose of calibrating the flow roughness, the process of water level of spring tide at dry season in 2016 was used in the model, while the flood process in August 29, 2018 ("2018.08") was applied for the model flood scenario validation. The result of model calibration and verification is displayed in Figs. 2 and 3, respectively. Based on the calculation of mean absolute difference and the root mean square, the difference of the calibration result between the model and prototype data is 7.97 and 9.38 cm, respectively. Furthermore, the verification result of the mean absolute difference and the root-mean-square difference are 5.94 and 6.82 cm, respectively. Generally, the difference is reasonable and acceptable for model study, the physical model is thus employed to simulate flood scenarios and to quantify the impacts of changing river regime on the flood stage in the SZR.

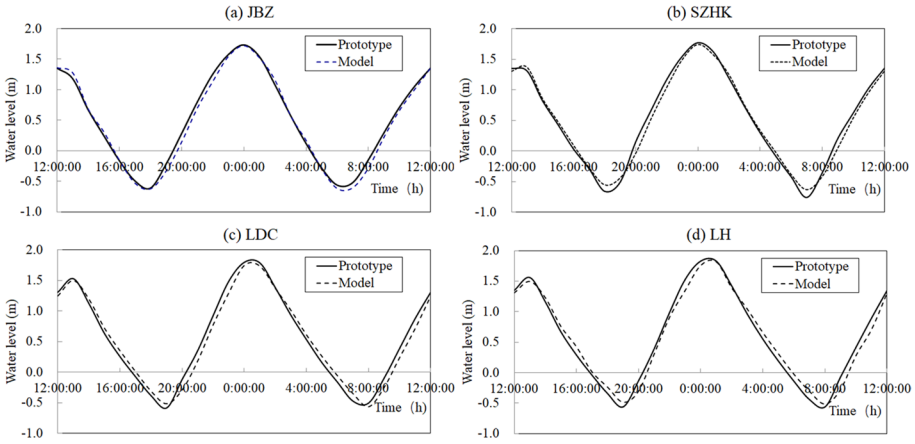

Fig. 2 Model calibration with flow process during the spring tide at dry season in 2016

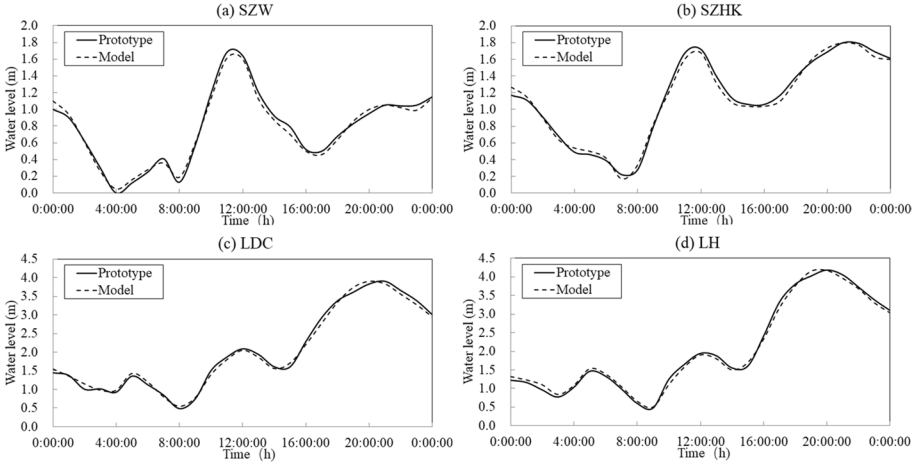

Fig. 3 Model validation with flow process at "2018.08" flood scenario

4 Increasing flood risk

4.1 Temporal variation of rainfall intensity

Generally, the short duration and high intensity rainstorm should be responsible for the flood event. In order to detect the temporal variation of regional rainfall, maximum 1 h rainfall intensity was collected from 2009 to 2017 at PYHK and LH stations (Fig. 4). Although maximum rainfall shows annual fluctuation, it is clear that the rainfall intensity presents obviously increasing trend, which seems to exacerbate the potential flood risk. At LH station, the maximum 1 h rainfall was 56 mm in 2009, while it reached 81.5 mm in 2017. The maximum 1 h rainfall increased by 45.5% in LH. Similar tendency can be found in PYHK station. The maximum 1 h rainfall intensity rises from 43.5 to 76 mm during the period of 2009–2017. Despite the precipitation regime can be distinct in different regions of the SZR basin, rainfall magnitude displays generally increasing trend, which probably triggered by climate change (Jian et al. 2020). Therefore, the occurrence possibility of flood event in the SZR increases. Furthermore, the synchronism of rainfall in different sub-basins is also highly intertwined with the potential flood risk.

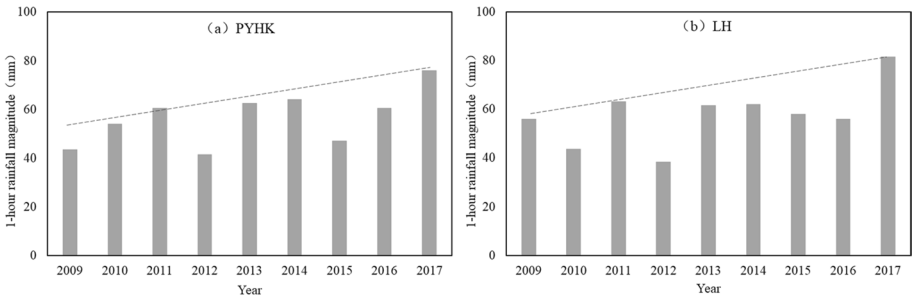

Fig. 4 Temporal variation of maximum 1 h rainfall intensity in **a** PYHK and **b** LH

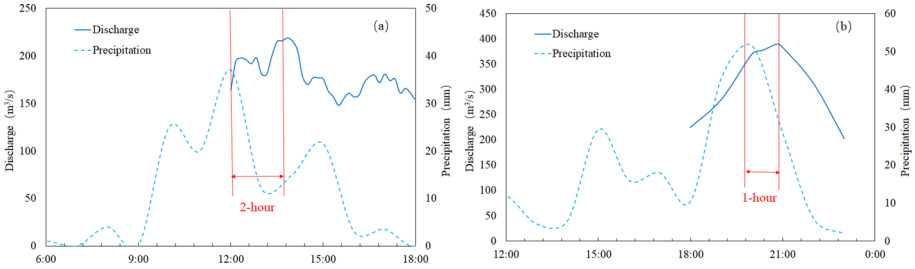

Fig. 5 The process of rainfall–runoff in **a** "2008.06" and **b** "2018.08" flood scenarios in LH station

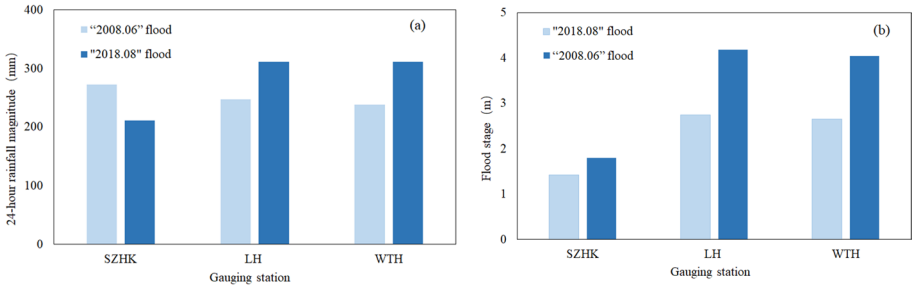

Fig. 6 The comparison of the "2008.06" and the "2018.08" scenarios in **a** 1 h rainfall magnitude and **b** flood stage

4.2 Changing rainfall–runoff duration

For the purpose of detecting the alteration of rainfall–runoff duration, processes of rainfall and runoff at June 13, 2008 flood ("2008.06") and August 29, 2018 flood ("2018.08") are compared (Fig. 5), both of which are the two most significant flood events with roughly equal magnitude in recent years in the SZR. For the "2008.06" flood, the occurrence of peak flood is about 2 h later than the peak rainfall in LH (Fig. 5a). However, during the period of the "2018.08" flood, the rainfall–runoff duration substantially shortens. The occurrence of peak flood is only 1 h later than the peak rainfall (Fig. 5b). Faster runoff generation and flow concentration are probably associated with characteristic of city underlying surface (Xu et al. 2021; Darby 1999). The farmland in the upper mainstream of the SZR basin mostly disappears due to the rapid urbanization process, as well as the water and soil conservation. Extensive urbanized land leads the buffering effect to be obviously undermined after rainstorm, which should be incorporated to account for shorter rainfall–runoff duration and increasing flood risk in the SZR.

4.3 Rising flood stage

Apart from the difference of rainfall–runoff duration, the flood stage is also distinct between the "2008.06" and "2018.08" flood. Actually, the rainfall magnitude of "2008.06" flood is nearly equal to the "2018.08" flood, taken the 24 h rainfall magnitude as an example. At SZHK station, rainfall magnitude of the "2008.06" flood is about 60 mm, which is

higher than the "2018.08" flood (Fig. 6a). Nevertheless, the 24 h rainfall magnitude of the "2008.06" flood is relatively lower at LH and WTH station, upstream the SZHK at Shenzhen and Hong Kong, respectively. Moreover, the two flood events are subject to similar tidal process. The peak flood encountered with the ebb tide, indicating that tidal motion exerts barely impact on the flood stage of the SZR. Unexpectedly, the flood stage of the "2018.08" flood is significantly higher than the "2008.06" flood (Fig. 6b). At SZHK, lower part of the SZR, the flood stage of the "2018.08" flood elevates about 0.4 m. At the upper part of the SZR, LH and WTH, the water level of the "2018.08" flood is about 1.4 m higher than the "2008.06" flood, which increases by nearly 50%. According to the secular hydrological data, the flood stage in the "2018.08" flood is the highest water level on records, although the precipitation magnitude has no obvious advantage comparing with the historical data.

5 Discussion

Generally, the increasing flood risk can be closely related to river channel regime (channel roughness, sediment deposition, channel width or shoreline changes), engineering facilities (bridge, wharf, sluice etc.), fluvial and coastal condition (runoff load variation, sea level rise). In the SZR, barely bridges or wharfs have been constructed as a result of the limitation of border river management in the past decades, indicating that no additional engineering facilities interfered with flood release. According to historical remote-sensing data, scarcely shoreline changes were found due to complete embankment construction after 2006. However, significant channel deposition emerged during the study period, accompanying with extensive riparian vegetation and estuarine mangrove forest developed in tidal flats, which probably enhances flood stage and improves flood release resistance. Moreover, Wu et al. (2020) found that the annual river flow in the SZR was relatively steady based on Mann–Kendall and Sen's slope estimator statistical tests, indicating that the runoff variation is only a minor contributor to flood risk. Therefore, only the impacts of riparian vegetation, estuarine mangrove forest, channel deposition and sea level rise on the SZR flood risk were further discussed.

5.1 Impact of riverine plant on the flood stage

In order to improve the flood protection ability of the SZR, river trainings have been conducted in different parts of branches since 1995, including the stage 1 and 2 downstream LH finished in 1999, and the stage 3 upstream LH finished in 2006. Since the riverbed has been significantly deepened by about 4–5 m, riverine flats were almost excavated in the early phase of river trainings (Wu et al. 2020). As continuous channel infilling, the range of tidal flat stepwise extended with plenty of riparian vegetation developed. Based on historical remote-sensing images in the SZR, it is clear to find tidal flats with dense riparian vegetation intensively evaded the channel during the period of 2003–2016 (Fig. 7). The boundary of riparian vegetation has expanded more than 30 m from the original bank into the river with obvious reduction of flood-carrying capacity, which probably improves the potential flood risk since the integrated channel roughness increases. Moreover, river plant is prevalent along the SZR. Especially on the middle and lower mainstream, tall riparian vegetation occupies about 80% branches along the riverside.

Fig. 7 Remote-sensing image of riverine vegetation in Feb-2003 (left) and Jul-2016 (right)

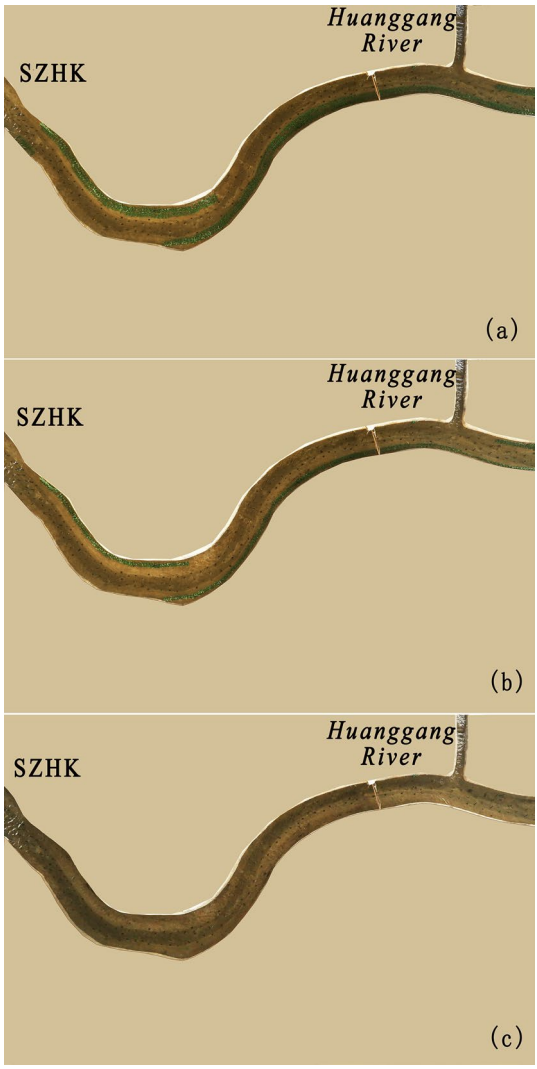

Fig. 8 Different range of vegetation in the physical model, including **a** all vegetation, **b** half vegetation and **c** no vegetation

The physical model is applied to study the impacts of riparian vegetation on the flood stage in this study. Three situations were modelled with different range of vegetation, including all vegetation (actual situation), half vegetation and no vegetation (Fig. 8). Flood stage variations were detected in 2-yr and 50-yr return period. Compared with all vegetation situation, the 50-yr flood stage may decrease by 0.09 m at average for half vegetation. Especially on the branch 4 km and 6 km away from the river mouth, flood stage obviously declines by more than 0.2 m, while it barely reduces upper 8 km, which is closely intertwined with the distribution of vegetation along the river. As for the flood with 2-yr return period, flood stage is hardly affected by vegetation, probably because lower flood stage is not able to submerge vegetation. All vegetation in actual situation can exert much more influence on the flood stage than the half vegetation condition (Fig. 9). The 50-yr flood stage for no vegetation is 0.43 m lower than all vegetation condition on average. Especially on the branch 4 km and 9 km away from the river mouth, the flood stage significantly declines by more than 0.6 m. The farther upstream 9 km, the less vegetation impact on the flood stage. Interestingly, near the river mouth, the flood stage for half and no vegetation condition has the potential to elevate, indicating that the water level gradient tends to be gentler with less riverine vegetation roughness.

According to the results of physical model, extended riverine plants are unfavourable for flood hazard prevention. Since riverine vegetation is considered a cause of river blockages by increasing the flow roughness especially during periods of high water levels (Fernandez et al. 2021), the flood stage then has the potential to rise due to larger flow resistance. Considering riverine vegetation unevenly distribute along the SZR, the impacts of riverine vegetation on the flood stage can be spatially different. The results find that the branch 4–9 km away from the river mouth presents larger flood stage increase, which associates well with the vegetation distribution. Based on the remote-sensing image, the branch 4–9 km away from the river mouth exhibits widespread and dense vegetation. From the perspective of flood prevention, vegetation should be removed in river management in order to avoid a cause of flooding. Actually, vegetation can also increase riverbank stability and reduce erosion by slowing down flow velocity primarily during low-flow periods (Croke et al. 2017). Furthermore, the interactions between vegetation, flow structure and sediment transport are conductive to the aquatic environment and ecosystem. Hence, some suggestions have been made to retain vegetation to avoid costly and ecologically damaging procedures of removing vegetation (Wang et al. 2015), which requires more reasonable river management and planning to balance flood prevention and healthy aquatic ecosystem (Symmank et al. 2020).

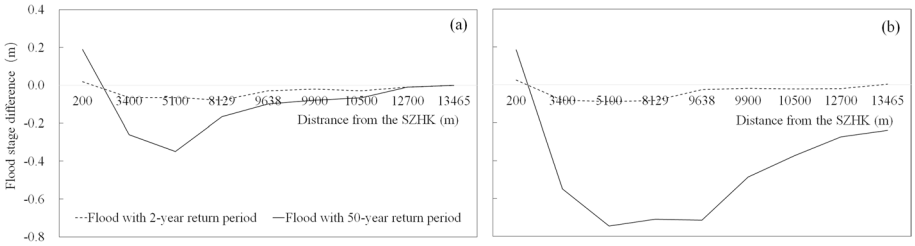

Fig. 9 Flood stage difference **a** between half vegetation and all vegetation, **b** between no vegetation and all vegetation in 2-year and 50-year flood return period

5.2 Impact of estuarine mangrove forest on the flood stage

Two parts of mangrove forests, Futian and Mipu mangrove nature reserves, locates near the river mouth of SZR, which may influence the flood process. The range of mangrove forest has continuously developed and extended in past two decades due to the well protection. According to the remote-sensing image, the area of Mipu mangrove reserve increases from 2.3 km^2 in 2002 to 3.5 km^2 in 2018. Especially close to the river mouth, the mangrove extended seaward by about 1 km. Furthermore, the Futian mangrove reserve almost doubles in area (0.43 km^2 in 2002 and 0.87 km^2 in 2018), which is obviously detrimental to flood release of the SZR. In order to study the impact of estuarine mangrove forest on the flood stage, the range of mangrove in 2002 and 2018 are selected to compare the flood stage alteration (Fig. 10).

Estuarine mangrove forest may hold back flood and then elevate the flood stage, primarily in the lower part of the SZR (Fig. 11). In the case of 200-yr return period flood, the flood stage increases by 0.28 m in 2018. However, the mangrove range exert much less influence in the middle and upper reaches. Upstream the 3 km away from the river mouth,

Fig. 10 Different range of estuarine mangrove in the physical model in **a** 2002 and in **b** 2018

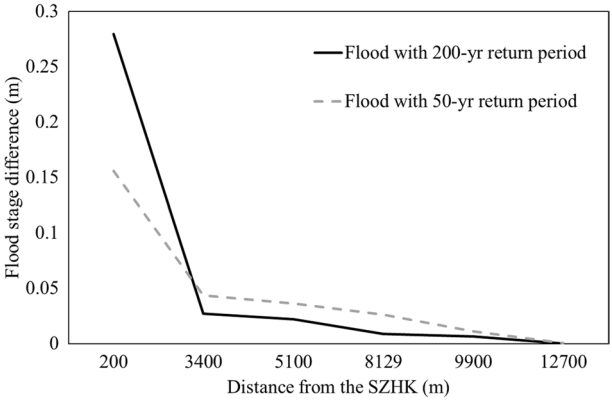

Fig. 11 Flood stage difference between mangrove range in 2002 and 2018 for 50-yr and 200-yr return period

barely flood stage difference between the mangrove range in 2002 and 2018 is found since the water level variation is lower than 0.02 m. The flood stage for the case of 50-yr return period displays similarly spatial variation. Compared with the mangrove range in 2002, large-scale mangrove forest in 2018 leads to about 0.15 m higher flood stage in the river mouth. The development of mangrove forest poses a challenge to the flow expansion in estuarine regions. The flow roughness is therefore increased, resulting in more interference on flood release and higher flood stage. Although mangrove forest plays an important role on the estuarine ecological environment system, as well as the buffering effect on undermining storm surge (Zhou et al. 2022; Chen et al. 2021), it needs to be limited if disordered growth happens for the consideration of flood risk. Potential flood risk driven by dense and large-scale mangrove should not be ignored in the estuarine management.

5.3 Riverbed elevation

In order to improve the flood prevention ability, a series of river trainings have been implemented in the past several decades in the SZR. The branch below LH was dredged to the design bed level before 2000, and the branch upper LH was dredged in 2006. After that, significant channel infilling emerged with continuous sediment accretion, driven by tidal asymmetry impacts with net sediment import and trapping. It is clear that the riverbed experiences obvious deposition (Fig. 12). The bed level increased by 0.5 m from 2002 to 2016 on average. In the lower reach of the LH, slighter deposition was found, while remarkable siltation occurred after 2007 in the upper reach. The riverbed upper LH rises by about 2 m during the period of 2007–2012. After 2012, the process of sediment siltation nearly ceased, since the continuous channel infilling undermined tidal asymmetry, leading to the gap between sediment import and export to be bridged. Hence, a near-equilibrium state was achieved after 2012 in the SZR (Wu et al. 2020).

Generally, water level is probably affected by the morphological change of riverbed. Flood capacity is decreased as channel aggradation occurs (Saad and Habib 2021). With equal fluvial discharge, water level increases as the riverbed elevates. Therefore, the flood stage can rise by about 0.5 m on the whole with channel infilling from 2002 to 2012 in the SZR. Since an equilibrium state has been obtained with hardly sediment deposition in the SZR after 2012, channel infilling would not be an important agent in controlling flood hazards of the SZR in the future. In low-gradient tidal river systems characterized by complex

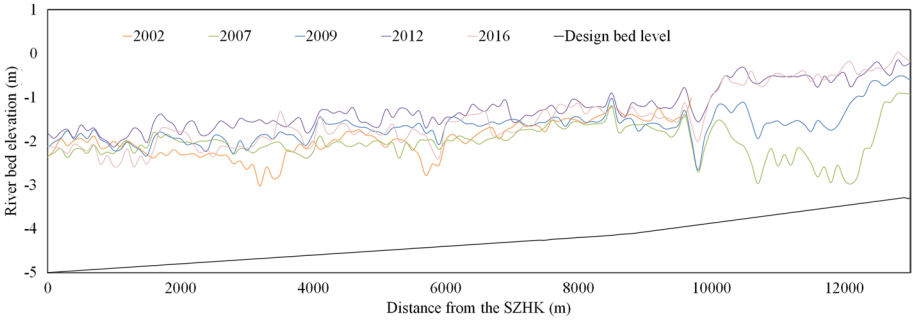

Fig. 12 Temporal variation of river bed elevation

reversal and bidirectional flows, large-scale channel modifications via riverine dredging exerts beneficial effect on fluvial flood prevention. Especially, dredging approaches that are extensive in spatial extent and modifications to channel longitudinal slope can result in obvious reductions in flood stages (Saad and Habib 2021). However, feedback between tidal dynamic, sediment transport and channel infilling promotes the tidal-dominant river system to evolve towards an equilibrium state. Flood prevention ability enhancement by dredging activities thus can be substantially undermined by river resilience in a short term, indicating that intensive river trainings should be ruled out in the SZR' further management strategy (Wu et al. 2020; Nones 2019).

5.4 Sea level rise

Sea level rise, a well-documented and urgent aspect of global warming, threatens population and assets located in low-lying coastal regions all around the world (Moftakhari et al. 2017; Dangendorf et al. 2015). Direct observations from tidal gauging stations and global satellite altimetry have shown that sea level is progressively rising (Passeri et al. 2015). Furthermore, the rate of sea level rise has increased in recent decades. Field-measured tidal data documents that the mean sea level rose at a rate of approximately 1.7 mm/year over the twentieth century, while it accelerated to a rate as high as approximately 3.4 mm/year after 1990s (Hay et al. 2015; Nerem et al. 2010). The sea level rise impacts such as increased coastal flooding, wetlands and wildlife habitat submergence, saltwater intrusion and shoreline erosion have been observed (Fitzgerald et al. 2008).

Tidal river systems vulnerable to sea level rise are at a risk for more flooding hazards due to the compounding impact of fluvial and coastal flooding. At the Shenzhen Estuary, the mean sea level has also inevitably increased. According to long-term tidal data at Chiwan (CW) station, variations in mean sea level have been detected. In Fig. 13, it is clear that the mean sea level increased by 0.16 m from 1964 to 2015, with an apparent acceleration after the 1990s. On the one hand, the direct influence of sea level rise on the SZR flood stage seems slow and gentle, probably less than 2 km near the river mouth, while the influence intensity can be cumulative. On the other hand, the associated effect, such as increasing tidal pumping, can be more detrimental. Physically, sea level rise has the potential to enable greater upstream tidal wave propagation (Guo et al. 2018), reducing pressure gradients that are important for transporting fluvial water then enhance flood risk (Hoitink and Jay 2016). Especially for tidal-dominant estuaries such as the SZR, the increase in tidal

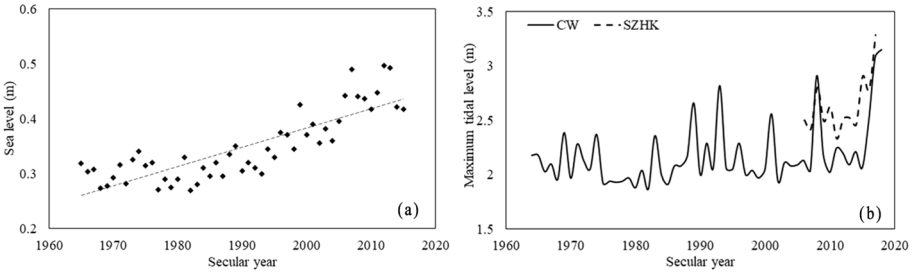

Fig. 13 Temporal variation of **a** mean sea level at the Shenzhen Estuary from 1964 to 2015 and **b** maximum tidal level in the CW and SZHK

pumping effect triggered by sea level rise can increase flood duration and flood stage in the middle and lower reaches. The nonstationarity introduced by sea level rise complicates fluvial flood (Buchanan et al. 2016), which needs further study.

Additionally, the intensity of storm surges associated with landfalling tropical cyclones has been reinforced due to climate change, which is also sensitive to sea level rise (Gao et al. 2014). Based on field-measured data at the estuarine region, the temporal variation of annual maximum tidal level is displayed after 1965, exhibiting a similar increasing trend after 1990 (Fig. 13). The highest tidal level record near the SZB was broken over and over again in recent years. Furthermore, sea level rise brings the height of high tides closer to flood stage, and increases the frequency of both nuisance floods (Vandenberg-Rodes et al. 2016; Moftakhari et al. 2016) and destructive flood events (Kemp and Horton 2014; Vousdoukas et al. 2017). Therefore, coastal cities like Shenzhen and Hong Kong should pay greater attention to the impact of sea level rise associated with extreme storm surges on flood prevention.

6 Conclusions

This study unravels changing flood pattern and evaluates possible influential factors in the tidal river system of the SZR. Based on the comparison of two typical flood scenarios in 2008 and 2018 with similar rainfall and tidal process, the flood stage significantly increases by about 1.4 m and the rainfall–runoff duration decreases by about 1 h in 2018. These changes indicate that the potential flood risk in the SZR has increased apparently in the past two decades, which is probably attributed to the extension of riverine vegetation, estuarine mangrove development and sediment deposition. The extensive and dense riverine vegetation, expanding more than 30 m along about 80% of the SZR, exerts a crucial control on the flood stage at the middle reach. Especially during the 50-yr return period, the flood stage obviously raised by more than 0.6 m compared with no vegetation condition. Large-scale floods are more susceptible to riverine vegetation with higher flow roughness. Moreover, the mangrove forest, which enlarged by 1.64 km^2 near the river mouth between 2002 and 2018, imposed less detrimental effects than riverine vegetation with about 0.2 m flood stage increment in the lower reach of the SZR. Additionally, continuous channel infilling with a magnitude of 0.5 m was observed after dredging activities since 2002, which probably contributed to the flood stage increase for all reaches. Understanding the influential factors and their degrees of impact on flood risk is essential for long-term river management

and flood hazard prevention. Most of the fast-growing riverine vegetation should be cleared before each wet season in case of unexpected high-level floods. Nevertheless, more deliberative management and planning on estuarine mangrove should be developed through further scientific research, since maintaining the balance between flood prevention and healthy aquatic ecosystem in estuarine regions often challenges policy makers. Considering that a dynamic equilibrium state has been obtained with hardly any sediment deposition in the SZR after 2012, channel infilling would not be an important factor influencing flood hazards in the SZR in the future. Regular topography surveys every few years can be incorporated in river management to monitor potential morphological changes. Sea level rise appears to be only a minor contributor to flood risk in the short term, but its cumulative impacts intertwined with extreme storm surge should not be ignored.

Acknowledgements This work was jointly supported by "National Natural Science Foundation of China" (NSFC, Project Nos. 42006157), The Belt and Road Special Foundation of the National Key Laboratory of Water Disaster Prevention (2020492111), The Open Research Fund of Key Laboratory of Sediment Science and Northern River Training, the Ministry of Water Resources, China Institute of Water Resources and Hydropower Research, (Grant NO. IWHR-SEDI-202105), the Science and Technology Planning Project of Guangzhou city, China (Project No. 202002030468).

Declarations

Conflict of interest The authors have no relevant financial or non-financial interests to disclose.

References

Buchanan MK, Kopp RE, Oppenheimer M, Tebaldi C (2016) Allowances for evolving coastal flood risk under uncertain local sea-level rise. Clim Change 137:347–362. https://doi.org/10.1007/s10584-016-1664-7

Chan SN, Lee JHW (2010) Impact of river training on the hydraulics of Shenzhen River. J Hydro-Environ Res 4:211–223. https://doi.org/10.1016/j.jher.2010.08.001

Chen Q, Li Y, Kelly DM, Zhang K, Zachry B, Rhome J (2021) Improved modeling of the role of mangroves in storm surge attenuation. Estuar Coast Shelf Sci 260:107515. https://doi.org/10.1016/j.ecss.2021.107515

Croke J, Thompson C, Fryirs K (2017) Prioritising the placement of riparian vegetation to reduce flood risk and end-of-catchment sediment yields: important considerations in hydrologically-variable regions. J Environ Manag 190:9–19. https://doi.org/10.1016/j.jenvman.2016.12.046

Dangendorf S, Marcos M, Müller A, Zorita E, Riva R, Berk K, Jensen J (2015) Detecting anthropogenic footprints in sea level rise. Nat Commun 6:7849. https://doi.org/10.1038/ncomms8849

Darby SE (1999) Effect of riparian vegetation on flow resistance and flood potential. J Hydraul Eng 125:443–454. https://doi.org/10.1061/(ASCE)0733-9429(1999)125:5(443)

Fan P, Li JC, Liu QQ, Singh VP (2008) Case study: influence of morphological changes on flooding in Jingjiang River. J Hydraul Eng 134:1757–1766. https://doi.org/10.1061/(ASCE)0733-9429(2008)134:12(1757)

Fathi-Moghadam M, Kashefipour M, Ebrahimi N, Emamgholizadeh S (2011) Physical and numerical modeling of submerged vegetation roughness in rivers and flood plains. J Hydrol Eng 16:858–864. https://doi.org/10.1061/(ASCE)HE.1943-5584.0000381

Fay PA, Kaufman DM, Nippert JB, Carlisle JD, Harper CW (2010) Changes in grassland ecosystem function due to extreme rainfall events: implications for responses to climate change. Glob Change Biol 14:1600–1608. https://doi.org/10.1111/j.1365-2486.2008.01605.x

Fernandez RL, Mclelland S, Parsons DR, Bodewes B (2021) Riparian vegetation life stages control the impact of flood sequencing on braided river morphodynamics. Earth Surf Process Landf 46:2315–2329. https://doi.org/10.1002/esp.5177

Fitzgerald DM, Fenster MS, Argow BA, Buynevich IV (2008) Coastal impacts due to sea-level rise. Annu Rev Earth Planet Sci 36:601–647. https://doi.org/10.1146/annurev.earth.35.031306.140139

Gao Y, Wang H, Liu G, Sun X, Fei X, Wang P, Lv T, Xue Z, He Y (2014) Risk assessment of tropical storm surges for coastal regions of China. J Geophys Res Atmos 119:5364–5374. https://doi.org/10.1002/2013JD021268

Gimbert F, Tsai VC, Lamb MP (2014) A physical model for seismic noise generation by turbulent flow in rivers. J Geophys Res Surf 119:2209–2238. https://doi.org/10.1002/2014JF003201

Guo L, Brand M, Sanders BF, Foufoula-Georgiou E, Stein ED (2018) Tidal asymmetry and residual sediment transport in a short tidal basin under sea level rise. Adv Water Resour 121:1–8. https://doi.org/10.1016/j.advwatres.2018.07.012

Hay CC, Morrow E, Kopp RE, Mitrovica JX (2015) Probabilistic reanalysis of twentieth-century sea-level rise. Nature 517:481–484. https://doi.org/10.1038/nature14093

He Y, Wu Y, Lu C, Wu M, Chen Y, Yang Y (2019) Morphological change of the mouth bar in relation to natural and anthropogenic interferences. Cont Shelf Res 175:42–52. https://doi.org/10.1016/j.csr.2019.01.015

Hey RD, Thorne CR (1986) Stable channels with mobile gravel beds. J Hydraul Eng 112:671–689. https://doi.org/10.1061/(ASCE)0733-9429(1986)112:8(671)

Hoitink AJF, Jay DA (2016) Tidal river dynamics: implications for deltas. Rev Geophys 54:240–272. https://doi.org/10.1002/2015RG000507

Jian W, Li S, Lai C, Wang Z, Cheng X, Lo EYM, Pan TC (2020) Evaluating pluvial flood hazard for highly urbanised cities: a case study of the Pearl River Delta Region in China. Nat Hazards 105:1691–1719. https://doi.org/10.1007/s11069-020-04372-3

Kemp AC, Horton BP (2014) Contribution of relative sea-level rise to historical hurricane flooding in New York City. J Quat Sci 28:537–541. https://doi.org/10.1002/jqs.2653

Kouwen N, Fathi-Moghadam M (2000) Friction factors for coniferous trees along rivers. J Hydraul Eng 126:732–740. https://doi.org/10.1061/(ASCE)0733-9429(2000)126:10(732)

Luo Z, Sun OJ, Xu H (2010) A comparison of species composition and stand structure between planted and natural mangrove forests in Shenzhen Bay, South China. J Plant Ecol 3:165–174. https://doi.org/10.1093/jpe/rtq004

Masterman R, Thorne CR (1994) Analytical approach to flow resistance in gravel-bed channels with vegetated banks

Moftakhari HR, Aghakouchak A, Sanders BF, Feldman DL, Sweet W, Matthew RA, Luke A (2016) Increased nuisance flooding along the coasts of the United States due to sea level rise. Past and future. Geophys Res Lett 42:9846–9852. https://doi.org/10.1002/2015GL066072

Moftakhari HR, Salvadori G, AghaKouchak A, Sanders BF, Matthew RA (2017) Compounding effects of sea level rise and fluvial flooding. Proc Natl Acad Sci U S A 114:9785–9790. https://doi.org/10.1073/pnas.1620325114

Nerem RS, Chambers DP, Choe C, Mitchum GT (2010) Estimating mean sea level change from the TOPEX and Jason altimeter missions. Mar Geodesy 33:435–446. https://doi.org/10.1080/01490419.2010.491031

Ng CN, Xie YJ, Yu XJ (2011) Measuring the spatio-temporal variation of habitat isolation due to rapid urbanization: a case study of the Shenzhen River cross-boundary catchment, China. Landsc Urban Plan 103:44–54. https://doi.org/10.1016/j.landurbplan.2011.05.011

Nones M (2019) Dealing with sediment transport in flood risk management. Acta Geophys 67:677–685. https://doi.org/10.1007/s11600-019-00273-7

Orton PM, Conticello FR, Cioffi F, Hall TM, Georgas N, Lall U, Blumberg AF, MacManus K (2018) Flood hazard assessment from storm tides, rain and sea level rise for a tidal river estuary. Nat Hazards 102:729–757. https://doi.org/10.1007/s11069-018-3251-x

Passeri DL, Hagen SC, Medeiros SC, Bilskie MV, Alizad K, Wang D (2015) The dynamic effects of sea level rise on low-gradient coastal landscapes: a review. Earth's Future 36:159–181. https://doi.org/10.1002/2015EF000298

Ralston DK, Talke S, Geyer WR, Al-Zubaidi HAM, Sommerfield CK (2019) Bigger tides, less flooding: effects of dredging on barotropic dynamics in a highly modified estuary. J Geophys Res: Oceans 124:196–211. https://doi.org/10.1029/2018JC014313

Ren H, Wu X, Ning T, Huang G, Wang J, Jian S, Lu H (2011) Wetland changes and mangrove restoration planning in Shenzhen Bay, Southern China. Landsc Ecol Eng 7:241–250. https://doi.org/10.1007/s11355-010-0126-z

Saad HA, Habib EH (2021) Assessment of riverine dredging impact on flooding in low-gradient coastal rivers using a hybrid 1D/2D hydrodynamic model. Front Water. https://doi.org/10.3389/frwa.2021.628829

Shimizu Y, Tsujimoto T (1994) Numerical analysis of turbulent open-channel flow over vegetation layer using a κ-ε turbulence model. J Hydrosci Hydraul Eng 11:57–67

Symmank L, Natho S, Scholz M, Schrder U, Schulz-Zunkel C (2020) The impact of bioengineering techniques for riverbank protection on ecosystem services of riparian zones. Ecol Eng 158:106040. https://doi.org/10.1016/j.ecoleng.2020.106040
Vandenberg-Rodes A, Moftakhari HR, Aghakouchak A, Shahbaba B, Sanders BF, Matthew RA (2016) Projecting nuisance flooding in a warming climate using generalized linear models and Gaussian processes. J Geophys Res: Oceans 121:8008–8020. https://doi.org/10.1002/2016JC012084
Vousdoukas MI, Mentaschi L, Voukouvalas E, Verlaan M, Feyen L (2017) Extreme sea levels on the rise along Europe's coasts. Earth's Future 5:304–323. https://doi.org/10.1002/2016EF000505
Vousdoukas MI, Mentaschi L, Voukouvalas E, Verlaan M, Jevrejeva S, Jackson LP, Feyen L (2018) Global probabilistic projections of extreme sea levels show intensification of coastal flood hazard. Nat Commun 9:2360. https://doi.org/10.1038/s41467-018-04692-w
Wang C, Zheng S, Wang P, Hou J (2015) Interactions between vegetation, water flow and sediment transport: a review. J Hydrodyn 27:24–37. https://doi.org/10.1016/S1001-6058(15)60453-X
Wang X, Xia J, Dong B, Zhou M, Deng S (2021) Spatiotemporal distribution of flood disasters in Asia and influencing factors in 1980–2019. Nat Hazards 108:2721–2738. https://doi.org/10.1007/S11069-021-04798-3
Wang Z, Feng Z, Chen P, Yi R, Tan G (2022) Evolution process of mangrove forests in Shenzhen Bay and its response to human activities. China Rural Water Hydropower 12:24–30 (**in Chinese**)
Wu Y, Zhang W, Zhu Y, Zheng J, Ji X, He Y, Xu Y (2018) Intra-tidal division of flow and suspended sediment at the first order junction of the Pearl River Network. Estuar Coast Shelf Sci 209:169–182. https://doi.org/10.1016/j.ecss.2018.05.030
Wu Y, He Y, Lu C, Zhang W, Gao S (2020) Feedback between channel resilience and tidal dynamics in an intensively dredged tidal river. J Hydrol 590:125367. https://doi.org/10.1016/j.jhydrol.2020.125367
Xie W, Wang X, Guo L, He Q, Dou S, Yu X (2021) Impacts of a storm on the erosion process of a tidal wetland in the Yellow River Delta. CATENA 205:105461. https://doi.org/10.1016/j.catena.2021.105461
Xu T, Xie Z, Zhao F, Li Y, Yang S, Zhang Y, Yin S, Chen S, Li X, Zhao S, Hou Z (2021) Permeability control and flood risk assessment of urban underlying surface: a case study of Runcheng south area, Kunming. Nat Hazards 111:661–686. https://doi.org/10.1007/S11069-021-05072-2
Zhang S, Mao X (2015) Hydrology, sediment circulation and long-term morphological changes in highly urbanized Shenzhen River estuary, China: a combined field experimental and modeling approach. J Hydrol 529:1562–1577. https://doi.org/10.1016/j.jhydrol.2015.08.027
Zhou X, Dai Z, Carniello L, Long C, Wang R, Luo J, Huang Z (2022) Linkage between mangrove wetland dynamics and wave attenuation during a storm–a case study of the Nanliu Delta, China. Mar Geol 454:106946. https://doi.org/10.1016/J.MARGEO.2022.106946

Authors and Affiliations

Yao Wu[1,2,3,4] · Wei Zhang[1,4] · Xiaozhang Hu[2,3] · Chen Lu[2,3,5] · Shiyou Gao[2,3]

✉ Yao Wu
wyaker@hotmail.com

[1] The National Key Laboratory of Water Disaster Prevention, Hohai University, Nanjing 210098, China

[2] Pearl River Water Resources Research Institute, Guangzhou 510610, China

[3] Key Laboratory of Pearl River Estuary Regulation and Protection, Guangzhou 510611, China

[4] College of Harbor, Coastal and Offshore Engineering, Hohai University, Nanjing 210098, China

[5] Southern Laboratory of Ocean Science and Engineering, Zhuhai 519082, China